Published for SISSA by Springer

Received: *January 8, 2013*
Accepted: *February 7, 2013*
Published: *March 5, 2013*

Higgs couplings beyond the standard model

Giacomo Cacciapaglia, Aldo Deandrea, Guillaume Drieu La Rochelle and Jean-Baptiste Flament

Université de Lyon, F-69622 Lyon, France; Université Lyon 1, Villeurbanne, CNRS/IN2P3, UMR5822, Institut de Physique Nucléaire de Lyon, F-69622 Villeurbanne Cedex, France

E-mail: g.cacciapaglia@ipnl.in2p3.fr, deandrea@ipnl.in2p3.fr, g.drieu-la-rochelle@ipnl.in2p3.fr, j-b.flament@ipnl.in2p3.fr

Abstract: We consider the Higgs boson decay processes and its production, and provide a parameterisation tailored for testing models of new physics beyond the Standard Model. We also compare our formalism to other existing parameterisations based on scaling factors in front of the couplings and to effective Lagrangian approaches. Different formalisms allow to best address different aspects of the Higgs boson physics. The choice of a particular parameterisation depends on a non-obvious balance of quantity and quality of the available experimental data, envisaged purpose for the parameterisation and degree of model independence, importance of the radiative corrections, scale at which new particles appear explicitly in the physical spectrum. At present only simple parameterisations with a limited number of fit parameters can be performed, but this situation will improve with the forthcoming experimental LHC data. Detailed fits can only be performed by the experimental collaborations at present, as the full information on the different decay modes is not completely available in the public domain. It is therefore important that different approaches are considered and that the most detailed information is made available to allow testing the different aspects of the Higgs boson physics and the possible hints beyond the Standard Model.

Keywords: Higgs Physics, Beyond Standard Model

ArXiv ePrint: 1210.8120

Open Access

doi:10.1007/JHEP03(2013)029

JHEP03(2013)029

Contents

JHEP03(2013)029

1 Higgs coupling parameterisations

The discovery of a new resonance at a mass of 125 GeV, announced by both ATLAS and CMS in July this year, has opened a new era in particle physics. In fact, the new particle has similar behaviour as the one expected for a Standard Model (SM) Higgs boson, and it has been observed in different channels, notably the decay into a pair of photons and into a pair of massive gauge bosons (ZZ and W^+W^-, where one of the two vectors is virtual). If confirmed, the discovery of the hard-sought SM Higgs boson would complete the picture for the Standard Model. However, intriguing discrepancies have also been observed, like for instance an excess in the di-photon rate and the non-observation of di-tau signal events by CMS. Such discrepancies are not statistically significant, thus they may disappear as mere statistical fluctuations. Even in this case, knowing the couplings of the new resonance is a crucial test for the SM hypothesis. Furthermore, many models of new physics, especially the ones addressing the problem of the hierarchy in the electroweak symmetry breaking sector, predict sizeable deviations in the Higgs couplings. Precise measurements of the Higgs properties, therefore, can give precious information on the kind of new physics that Nature chose. The information that can be extracted at the LHC is rather limited to a few channels, nevertheless it is important to make the best out of it. In the light of this consideration, it is important to choose the most relevant parameterisations for the deviations from the SM couplings, and use them to present the LHC measurements. Higgs coupling parameterisations, meant to perform fits on the available data, may follow different approaches which are not completely independent. In the following we will discuss a few

of them without aiming at an exhaustive description. We shall then discuss our suggestion which is particularly motivated by testing models Beyond the Standard Model (BSM).

From the experimental point of view it makes sense to just parameterise Higgs physics in terms of observed quantities such as branching ratios and cross-sections. This is for example the case of the parameterisation proposed in ref. [1], where the relevant cross-sections and partial decay widths are multiplied by a suitable factor. The advantage of such an approach is its simple link to the experimentally measured quantities. On the other hand, with such a choice, correlations among the different parameters are not explicit, in particular between tree level and loop induced observables. For example, a modification of the couplings to W bosons and top, while modifying tree-level branching ratios and cross-sections for the Higgs boson, can also affect the loop-level couplings for the Higgs production via the gluon channel or the Higgs decay into two photons. This is in principle not a limitation, but in practice if one wants to take these correlations into account a different choice of parameters needs to be considered. Another point is: what if, instead of a generic fit, one aims at discussing limits for a particular BSM model? In that case explicit correlations among the fit parameters should be calculated in order to correctly compute the number of independent degrees of freedom for the fit. Therefore, a parameterisation which can easily be connected to any model of new physics is also useful. Along these lines, we propose an extension of the parameterisation in ref. [2], where the contribution of loops of New Physics to the $H \to gg$ and $H \to \gamma\gamma$ modes is explicitly disentangled from the modification of tree level couplings, thus removing correlations among the various parameters. Furthermore, the loop contributions are normalised to the top ones, thus simplifying the interpretation in terms of new models.

Another point of view consists in parameterising physics in terms of effective operators (for a specific strategy concerning the Higgs boson data and the interpretation in terms of physics beyond the Standard Model see [3–5]). Another example is given by chiral electroweak Lagrangians [6, 7]. This approach has the advantage of inheriting all the standard know-how in effective theories, including the calculation of radiative corrections. The possible remarks to such an approach is the large number of effective couplings when going beyond the lowest order set and the treatment of possible light degrees of freedom beyond the SM particles (this possibility is not completely ruled out as particles in the same mass range as the SM Higgs boson might still be possible, see for example [8]). A quite detailed and clearly written overview of effective Lagrangians for Higgs physics is given in [9], including the treatment of radiative corrections.

The question of the choice of a parameterisation does not only depend on the particular use or preference for a given formalism, but also depends crucially on the number of fit parameters with respect to the number of physically independent data channels. In the frequentist approach one computes a χ^2 per degree of freedom within a given choice of model (with a given number of independent fit parameters). The choice of a particular fit "model" is a matter of a reasonable rule of thumb, as too many fit parameters compared to too few experimental data channels give a poor quality fit.[1]

[1] "With four parameters I can fit an elephant, and with five I can make him wiggle his trunk". Rule of thumb attributed to John von Neumann by Enrico Fermi, as quoted by Freeman Dyson in "A meeting with Enrico Fermi" in Nature 427 (January 2004) p. 297.

JHEP03(2013)029

In the following we wish to discuss how the parameterisation of the Higgs couplings to gluons and photons proposed in ref. [2] can be extended to include tree level couplings modifications, and how it compares to other parameterisations, in particular the one proposed in ref. [1]. A similar study has also been recently carried out in [10]. We will try to show that the extension of [2] is especially useful when the results of a fit on the parameters are to be interpreted in terms of specific models of new physics beyond the standard model. For the tree level couplings, we follow the same parameterisation as in table 2 of ref. [1], i.e. we introduce a scaling factor in front of the coupling, κ_X where X is any massive particle of the SM the Higgs couples directly to. The same scaling factor will appear in front of some cross sections and partial decay widths. For example:

$$\sigma_{Wh} = \kappa_W^2 \sigma_{Wh}^{\rm SM}\,, \quad \sigma_{Zh} = \kappa_Z^2 \sigma_{Zh}^{\rm SM}\,, \quad \sigma_{t\bar{t}h} = \kappa_t^2 \sigma_{t\bar{t}h}^{\rm SM}\,. \tag{1.1}$$

For the partial decay widths:

$$\Gamma_{WW} = \kappa_W^2 \Gamma_{WW}^{\rm SM}\,, \quad \Gamma_{ZZ} = \kappa_Z^2 \Gamma_{ZZ}^{\rm SM}\,, \quad \Gamma_{b\bar{b}} = \kappa_b^2 \Gamma_{b\bar{b}}^{\rm SM}\,, \quad \Gamma_{\tau^+\tau^-} = \kappa_\tau^2 \Gamma_{\tau^+\tau^-}^{\rm SM}\,, \ldots \tag{1.2}$$

For the Vector Boson Fusion (VBF) cross sections, it is imperative to distinguish the two production channels with W or Z fusion:

$$\sigma_{VBF} = \kappa_W^2 \sigma_{WF}^{\rm SM} + \kappa_Z^2 \sigma_{ZF}^{\rm SM}\,. \tag{1.3}$$

So far, the parameterisation is the same as in ref. [1]: the crucial differences arise in the treatment of loop induced couplings, as explained in the following section.

2 Loop induced couplings: κ_{gg} and $\kappa_{\gamma\gamma}$ vs. κ_g and κ_γ

The parameters introduced so far describe tree level couplings of the Higgs. Typically, sizeable modification to such couplings are generated by tree level effects from New Physics, like for example mixing of the SM particles with heavier states. Modifications of the loop induced couplings, however, deserve a different treatment, because they are directly sensitive to any new state that may enter the loop. In ref. [1], a scaling parameter was also introduced to describe the new physics effects in the couplings to gluons and photons, namely:

$$\sigma_{ggH} = \kappa_g^2 \sigma_{ggH}^{\rm SM}\,, \quad \Gamma_{gg} = \kappa_g^2 \Gamma_{gg}^{\rm SM}\,, \quad \Gamma_{\gamma\gamma} = \kappa_\gamma^2 \Gamma_{\gamma\gamma}^{\rm SM}\,. \tag{2.1}$$

However, both κ_g and κ_γ depend non trivially on the tree level couplings, in particular κ_W and κ_t, because a modification of the couplings to W and tops would affect the SM loop contribution to the couplings to gluons and photons. So, in general, there is a correlation intrinsic in this scaling parameter approach.

On the contrary, in ref. [2], we proposed an alternative parameterisation of the couplings to gluons and photons that can deal with loop corrections from new physics in an independent way from the tree level corrections to the couplings to massive SM states. In this way, the parameters are not correlated to each other. Note that a parameterisation equivalent to the one we present here has been recently and independently used in [11].

JHEP03(2013)029

Furthermore, our parameterisation allows to obtain bounds that are more easily interpreted in terms of new physics models. The new parameters, κ_{gg} and $\kappa_{\gamma\gamma}$, enter at the level of the amplitude of the loop corrections. In terms of the partial decay widths, we have:

$$\Gamma_{\gamma\gamma} = \frac{G_F \alpha^2 m_H^3}{128\sqrt{2}\pi^3} \left| \kappa_W A_W(\tau_W) + C_t^\gamma \, 3 \left(\frac{2}{3}\right)^2 A_t(\tau_t) \, [\kappa_t + \kappa_{\gamma\gamma}] + \dots \right|^2 , \tag{2.2}$$

$$\Gamma_{gg} = \frac{G_F \alpha_s^2 m_H^3}{16\sqrt{2}\pi^3} \left| C_t^g \frac{1}{2} A_t(\tau_t) \, [\kappa_t + \kappa_{gg}] + \dots \right|^2 , \tag{2.3}$$

where the dots stand for the negligible contribution of the light quarks. The coefficients C_t^γ and C_t^g contain the NLO QCD corrections to the SM amplitudes. A_W and A_t are the well known W and top amplitudes:

$$A_t(\tau) = \frac{2}{\tau^2} \left(\tau + (\tau - 1) f(\tau)\right) , \tag{2.4}$$

$$A_W(\tau) = -\frac{1}{\tau^2} \left(2\tau^2 + 3\tau + 3(2\tau - 1) f(\tau)\right) , \tag{2.5}$$

where $\tau = \frac{m_H^2}{4m^2}$ and

$$f(\tau) = \begin{cases} \arcsin^2 \sqrt{\tau} & \tau \leq 1 \\ -\frac{1}{4} \left[\log \frac{1 + \sqrt{1 - \tau^{-1}}}{1 - \sqrt{1 - \tau^{-1}}} - i\pi \right]^2 & \tau > 1 \end{cases} . \tag{2.6}$$

The amplitudes A_W and A_t have the property that they rapidly asymptotise to a constant value for large masses of the states inside the loop, i.e. for small τ. For a Higgs mass of 125 GeV, we find:

$$A_W(\tau_W) = -8.32 , \qquad A_t(\tau_t) = 1.37 ; \tag{2.7}$$

where the top amplitude is very close to its asymptotic value $A_t(0) = 4/3 \sim 1.33$. The W amplitude however significantly deviates from the asymptotic value $A_W(0) = -7$. The QCD corrections to the top loops can also be computed in the asymptotic limit of large top mass, which gives a good approximation of the much more complicated mass dependent corrections. One finds [12]:

$$C_t^\gamma = 1 - \frac{\alpha_s}{\pi} , \qquad C_t^g = 1 + \frac{9}{2} \frac{\alpha_s}{\pi} . \tag{2.8}$$

In the case of the gluon loop, the corrections, which also includes real emission of an additional gluon and splitting into a pair of light quarks, reduces to this simple form if α_s entering the LO amplitude is evaluated at the renormalisation scale $\mu = e^{-7/4} m_H \sim 22$ GeV: in other words, part of the correction is encoded in the running of the coupling constant. A more detailed discussion of the QCD corrections that can be included in this parameterisation will be discussed in a following section.

The original simplified parameterisation of [2] can be recovered setting the NLO coefficients C_t^γ and C_t^g to one and $\kappa_W = 1$, $\kappa_t = 1$. Note that the contribution of κ_t and κ_W

JHEP03(2013)029

was effectively included into the loop parameters, and we will discuss in more detail later in which case this procedure is allowed. We have normalised the contribution of the new physics loops to the contribution of the top loop alone. This is important when we want to interpret the fit of the parameters in terms of the properties and nature of the new physics running into the loop.

Neglecting the contribution of light fermions, we can draw a relation between the parameterisation [1] and ours:

$$\kappa_g(\kappa_t, \kappa_{gg}) = |\kappa_t + \kappa_{gg}| \,, \tag{2.9}$$

$$\kappa_\gamma(\kappa_W, \kappa_t, \kappa_{\gamma\gamma}) = \left| \frac{\kappa_W \, A_W(\tau_W) + C_t^\gamma \frac{4}{3} A_t(\tau_t) \, [\kappa_t + \kappa_{\gamma\gamma}]}{A_W(\tau_W) + C_t^\gamma \frac{4}{3} A_t(\tau_t)} \right| . \tag{2.10}$$

These formulas show clearly the correlation between the parameters. This correlation is absent in our proposed parameterisation.

3 Data analysis

The data analysed by the two collaborations (ATLAS and CMS) is presented in terms of measured cross sections in the relevant decay channels and for various selection rules: in the following, we will make use of as much information as it is available. For instance, for the $H \to \gamma\gamma$ channel, the measured signal is available for several selection cuts, while for $H \to ZZ \to 2 \times (l^+ l^-)$ and $H \to WW$, only the total measured cross section is available. In the case of the WW channel, the searches are actually performed in various selection channels, however the detailed efficiency of each signal region for the various production mechanisms is not publicly available. As in our parameterisation the contribution of the production channels to the total cross section is modified with respect to the SM, a meaningful fit is not possible without detailed information on the efficiencies. In a first step we will focus on the channels where all needed information is provided, $\gamma\gamma$, ZZ, $\bar{b}b$, and we will afterwards present a method to include also the WW and $\bar{\tau}\tau$ channels.

In general, for each selection channel i of the experiments, the data being fitted is represented by the best fit values of the signal strength $\hat{\mu}_i$ (defined as the observed number of events divided by the expected number of events for a SM Higgs boson) as well as its uncertainty σ_i. As described in [13], to compare these values to theoretical expectations, the signal strength in one channel must be compared to the one calculated in each model, given for a specific channel by:

$$\mu_i = \frac{n_s^i}{(n_s^i)^{\rm SM}} = \frac{\sum_p \sigma_p \, \epsilon_p^i}{\sum_p \sigma_p^{\rm SM} \epsilon_p^i} \times \frac{BR_i}{BR_i^{\rm SM}} \,, \tag{3.1}$$

where n_s^i is the predicted number of signal events in channel i in the studied model, and $(n_s^i)^{\rm SM}$ that same number in the SM. For each production mode p (theoretical calculation at NLO) the efficiency of selection of a channel i (experimental observation) is given by ϵ_p^i, considered to stay the same with new physics. This assumption is in agreement with our parameterisation that only includes corrections that do not change the kinematics of the

JHEP03(2013)029

Selection channel	$\hat{\sigma}^i_{gg}$	$\hat{\sigma}^i_{VBF}$	$\hat{\sigma}^i_{VH}$	$\hat{\mu}_i$	σ_i	$\hat{\sigma}^i_{gg}$	$\hat{\sigma}^i_{VBF}$	$\hat{\sigma}^i_{VH}$	$\hat{\mu}_i$	σ_i
	7 TeV					8 TeV				
Untagged 0	61	17	19	3.15	1.82	68	12	16	1.46	1.24
Untagged 1	88	6	6	0.66	0.95	88	6	6	1.51	1.03
Untagged 2	91	4	4	0.73	1.15	92	4	3	0.95	1.15
Untagged 3	91	4	4	1.53	1.61	92	4	3	3.78	1.77
Dijet Tag	27	73	1	4.21	2.04	—	—	—	—	—
Dijet tight	—	—	—	—	—	23	77	0	1.32	1.57
Dijet loose	—	—	—	—	—	53	45	2	-0.61	2.03

Table 1. CMS results in the $H \to \gamma\gamma$ channel [14, 15].

events. At last, BR_i and $BR_i^{\rm SM}$ are the branching ratios of the Higgs boson into the decay channel corresponding to the selection channel i, for both SM and studied model.

The following data have been used for each channels:

- $H \to \gamma\gamma$: in CMS, information was given in [14]: in table 2 of the reference, one can find the product $\hat{\sigma}^i_p = (\sigma^{\rm SM}_p \epsilon^i_p)/(\sum_{p'} \sigma^{\rm SM}_{p'} \epsilon^i_{p'})$ for each selection and production channel, whereas the best fit values as well as the uncertainties can be found in another table on the corresponding TWiki [15], for a Higgs mass of $m_H = 125\,\text{GeV}$. Those results are shown in table 1. The results from the ATLAS collaboration, on the other hand, can be found in note [16], where the selection channel efficiencies are given in table 6, and the best fit values had to be extracted from figures 14a and 14b for 7 TeV and 8 TeV respectively. They are shown in table 2.

- $H \to ZZ^* \to \ell^+\ell^-\ell^+\ell^-$: in this case, no tables were given by either experiment and we had to assume identical cut efficiencies for all production channels. This seems to be a reasonable assumption for an inclusive channel like ZZ, however this may not be the case if discriminants based on the kinematic properties of the leptons are used, as it is the case for CMS, where different efficiencies for different production channels may arise. The assumption of universal efficiency allowed us to replace the efficiency-scaled cross sections $\hat{\sigma}^i_p$ by standard cross sections σ_p, which were taken from the LHC Higgs Cross-section Working Group's Website [17]. Best fit values and uncertainties were extracted from figure 19 in [18], and figure 16a from the note [19], and the results are presented in table 3.

- $H \to \bar{b}b$: The most sensitive part[2] comes only through VH production, thus one can set all other efficiencies to zero, and the efficiency of the VH production cancels out in the ratio in eq. (3.1). The experimental results are $\hat{\mu} = -0.4 \pm 1.1$ for ATLAS and $\hat{\mu} = 1.3 \pm 0.7$ for CMS ([20, 21]).

[2]This final state is indeed also looked for in the $\bar{t}tH$ production, but the sensitivity is still low at the time being.

JHEP03(2013)029

Selection channel	$\hat{\sigma}^i_{gg}$	$\hat{\sigma}^i_{VBF}$	$\hat{\sigma}^i_{WH}$	$\hat{\sigma}^i_{ZH}$	$\hat{\mu}_i$	σ_i	$\hat{\sigma}^i_{gg}$	$\hat{\sigma}^i_{VBF}$	$\hat{\sigma}^i_{WH}$	$\hat{\sigma}^i_{ZH}$	$\hat{\mu}_i$	σ_i
	7 TeV						8 TeV					
Unconverted central low p_{Tt}	92.9	4.0	1.8	1	0.5	1.4	92.9	4.2	1.7	1.0	1.0	1.2
Unconverted central high p_{Tt}	66.5	15.7	9.9	5.7	0.2	1.9	72.5	14.1	6.9	4.2	0.8	1.7
Unconverted rest low p_{Tt}	92.8	3.9	2.0	1.1	2.4	1.6	92.5	4.1	2	1.1	0.9	1.4
Unconverted rest high p_{Tt}	65.4	16.1	10.8	6.1	10.3	3.8	72.1	13.8	7.8	4.6	1.8	1.8
Converted central low p_{Tt}	92.8	4.0	1.9	1.0	6.2	2.6	92.8	4.3	1.7	1.0	3.4	2.0
Converted central high p_{Tt}	66.6	15.3	10	5.7	-4.4	1.6	72.7	13.7	7.1	4.1	3.5	2.7
Converted rest low p_{Tt}	92.8	3.8	2.0	1.1	2.7	2.2	92.5	4.2	2	1.1	0.4	1.8
Converted rest high p_{Tt}	65.3	16.0	11.0	5.9	-1.7	3	70.8	14.4	8.3	4.7	0.3	2.1
Converted transition	89.4	5.2	3.3	1.7	0.3	3.7	88.8	6.0	3.1	1.8	5.5	3.3
2 jets	22.5	76.7	0.4	0.2	2.7	1.9	30.4	68.4	0.4	0.2	2.6	1.8

Table 2. ATLAS results in the $H \to \gamma\gamma$ channel [16].

Experiment	$\sigma_{gg}[pb]$	$\sigma_{VBF}[pb]$	$\sigma_{WH}[pb]$	$\sigma_{ZH}[pb]$	$\sigma_{tth}[pb]$	$\hat{\mu}$	σ
CMS ZZ	15.32	1.222	0.5729	0.3158	0.08634	0.8	0.35
ATLAS ZZ						1.3	0.6

Table 3. CMS and ATLAS results in the $H \to ZZ \to \ell^+\ell^-\ell^+\ell^-$ channel [18, 19].

When combining with our procedure the $\gamma\gamma$ ATLAS results, we met a problem with selection channel *Converted central high* p_{Tt}. Whereas for all the other channels the combination of 7 TeV and 8 TeV data gave results in agreement with the ones reported in figure 14c in [16], it was not the case for this channel. We therefore decided to ignore it in 7 TeV as well as 8 TeV data: the following ATLAS plots are combination of all remaining channels.

To fit our parameterisation, we used a χ^2 method where each computed signal strength is compared to its corresponding data best fit value through

$$\chi^2 = \sum_i \frac{(\mu_i - \hat{\mu}_i)^2}{\sigma_i^2} \,. \tag{3.2}$$

The values of χ^2 computed this way are then compared to the exclusion thresholds at 68 and 95% CL for a m degrees of freedom χ^2 distribution, where m is the number of channels i minus the number of independent fitted parameters (i.e. the number of independent parameters which value are fitted to the data).

JHEP03(2013)029

Canal	$(\hat{\mu}_{ggH/\bar{t}tH},\ \hat{\mu}_{i,VBF/VH})$	V
$H \to \gamma\gamma$	$(0.95,\ 3.77)$	$\begin{pmatrix} 0.95 & -1.35 \\ -1.35 & 6.87 \end{pmatrix}$
$H \to WW$	$(0.77,\ 0.39)$	$\begin{pmatrix} 0.19 & 0.15 \\ 0.15 & 1.79 \end{pmatrix}$
$H \to \tau\tau$	$(0.93,\ 0.89)$	$\begin{pmatrix} 2.02 & -0.92 \\ -0.92 & 2.14 \end{pmatrix}$

Table 4. CMS results in the $H \to WW$, $H \to \tau\tau$ and $H \to \gamma\gamma$ channels. Results inferred from [22], using equation (3.3).

3.1 Improved χ^2 method

As mentioned previously, the χ^2 obtained in eq. (3.2) meets two serious obstacles: first, one needs the efficiency (or equivalently the signal sample composition) per production mode together with the best fit $\hat{\mu}_i$ in each sub-channel and, second, this procedure neglects the correlations between uncertainties of the different sub-channels. However, it is possible to go further by recasting the results of the couplings analyses made by the two collaborations [22, 23]. Indeed, instead of providing the best fits as one dimensional distributions $(\hat{\mu}_i \pm \sigma_i)$, we now have access to two dimensional distributions $((\hat{\mu}_{i,ggH/\bar{t}tH}, \hat{\mu}_{i,VBF/VH})$, with the one sigma contour). Under some acceptable assumptions, this information can be used as the χ^2_i function of the channel i, without explicit reference to sub-channels and efficiencies. Those assumptions are the following:

- VBF and VH production are rescaled in the same way. This is achieved by imposing $\kappa_Z = \kappa_W$, which is the case in any model respecting the custodial symmetry.
- For each channel i, there cannot be significant contributions from both the gluon fusion and the t quark associated production. At the time being, this is the case, since $\bar{t}tH$ is significant only in the $H \to \bar{b}b$ channel which is otherwise observable only through VH.

As for the previous method, we must also assume that the Gaussian approximation is well motivated. We can then write the approximated likelihood of a given channel i as

$$\chi^2_i = \begin{pmatrix} \mu_{i,ggH/\bar{t}tH} - \hat{\mu}_{i,ggH/\bar{t}tH} \\ \mu_{i,VBF/VH} - \hat{\mu}_{i,VBF/VH} \end{pmatrix}^T V_i^{-1} \begin{pmatrix} \mu_{i,ggH/\bar{t}tH} - \hat{\mu}_{i,ggH/\bar{t}tH} \\ \mu_{i,VBF/VH} - \hat{\mu}_{i,VBF/VH} \end{pmatrix}, \tag{3.3}$$

which is nothing but the 2D version for eq. (3.2), where V_i and $\hat{\mu}_{i,X}$ are obtained by fitting the one sigma contour to $\chi^2_i(1\sigma) = 2.3$ (this value correspond to the 68% CL of a two-dimensional χ^2 distribution), see figures in table 4. The main difference with the 1D version is that we do not get directly the χ^2_i function, which *a priori* does not vanish anywhere, but its deviation to the best fit $\Delta\chi^2_i$ which vanishes at the best fit point. However we have checked that the resulting statistical test yields a conservative result as compared to the true χ^2 test, as long as each best value $\chi^2_i(\hat{\kappa})$ had a large p-value (i.e. not negligible as compared to one).

JHEP03(2013)029

We have mainly used this improved χ^2 for the CMS results, since all[3] channels could be treated this way, whereas the update of the WW channel in ATLAS did not include this information. Given that the uncertainties are so far statistically dominated, they are mostly uncorrelated hence we do not expect significant differences with the previous method, which we have checked by comparing the two methods on the same $H \to \gamma\gamma$ analysis from CMS. However this method is crucial for channels where efficiencies are not available (for instance the WW) and it may also be promising when the correlations become important in uncertainties.

In the following sections, we will use our reconstructed likelihood to derive confidence regions in our parameter space. This requires the choice of a statistical test, and we have compared two different tests. The first is the profiled likelihood ratio, i.e. the quantity $\Delta\chi^2(\kappa) = \chi^2(\kappa) - \chi^2(\hat{\kappa})$ and the second is the full χ^2 test. They differ in the sense that the $\Delta\chi^2$ test is the assessment of a given hypothesis (κ) as compared to another hypothesis ($\hat{\kappa}$), whereas the χ^2 test assesses the κ hypothesis without reference to other hypotheses. Depending on the data, they will have a different power: in general the $\Delta\chi^2$ will be stronger as long as the best fit $\hat{\kappa}$ is sufficiently likely; if this is not the case, then the χ^2 test should be used. This can be understood as the fact that the $\Delta\chi^2$ does not test whether a given choice of the parameters κ suitably describes the data, however it tests how a given point in the parameter space compares to the best fit point $\hat{\kappa}$. In the following sub-sections we present some sample fits, where we have chosen the most appropriate test case by case.

3.2 Simple two parameter fit

To start with, one can restrict the fit to the two parameters describing the loop couplings only. This can be justified in two cases:

- new physics only enters via loops, while corrections to tree level couplings are small;
- the most sensitive measurements only involve loop induced couplings, while the effects on tree level processes are subleading.

In the second case, one can absorb the contribution of κ_t and κ_W into the loop parameters:

$$\kappa'_{gg} = \kappa_{gg} + \kappa_t - 1\,, \tag{3.4}$$

$$\kappa'_{\gamma\gamma} = \kappa_{\gamma\gamma} + \kappa_t - 1 + \frac{3A_W}{4A_t}(\kappa_W - 1)\,. \tag{3.5}$$

Note for example that the $t\bar{t}h$ coupling is not measurable at the moment, thus κ_t can always be absorbed in κ_{gg} and $\kappa_{\gamma\gamma}$. Furthermore, a small contribution to $\kappa_W - 1$ can generate sizeable effects on $\kappa_{\gamma\gamma}$ due to the enhancement factor $\frac{3A_W}{4A_t} \sim -4.6$. In practice, present experimental results allow to perform a meaningful fit only with a very restricted set of parameters. This relation is also in agreement with the expectation that modifications to the tree level couplings, κ_W and κ_t, are generated by New Physics effects at tree level.

[3]Of course there is no need for such a treatment in the ZZ channel, since it does not distinguish productions modes.

JHEP03(2013)029

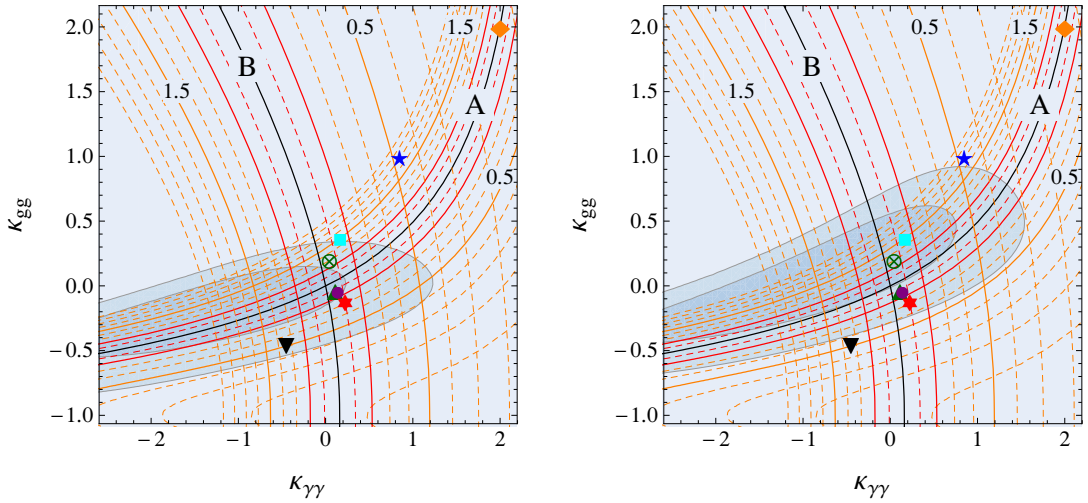

Figure 1. $\kappa'_{\gamma\gamma}$ and κ'_{gg} at the LHC for a Higgs boson with $m_H = 125\,\text{GeV}$. The two solid lines correspond to the SM values of the inclusive $\gamma\gamma$ channel (**A**), and the vector boson fusion production channel (**B**). On the left panel, the fit using ATLAS data. On the right, the fit using CMS data. Both fits use $\gamma\gamma$, ZZ and $\bar{b}b$ channels. Darker (lighter) blue are the 1, 2 σ limits.

In the two parameter case [2], the signal strength can be calculated with all given data, as the cross sections for each production channel is proportional to the one in the SM. We can therefore write for the $H \to \gamma\gamma$ channels:

$$\begin{aligned}\mu_{i,\,\gamma\gamma} &= \frac{(1+\kappa_{gg})^2\sigma^{\rm SM}_{gg}\epsilon^i_{gg} + \sigma^{\rm SM}_{VBF}\epsilon^i_{VBF} + \sigma^{\rm SM}_{ZH}\epsilon^i_{ZH} + \sigma^{\rm SM}_{WH}\epsilon^i_{WH}}{\sigma^{\rm SM}_{gg}\epsilon^i_{gg} + \sigma^{\rm SM}_{VBF}\epsilon^i_{VBF} + \sigma^{\rm SM}_{ZH}\epsilon^i_{ZH} + \sigma^{\rm SM}_{WH}\epsilon^i_{WH}} \times \frac{BR_{\gamma\gamma}}{BR^{\rm SM}_{\gamma\gamma}} \\ &= \frac{1+\left[(1+\kappa_{gg})^2-1\right]\hat{\sigma}^i_{gg}}{1+\left[(1+\kappa_{gg})^2-1\right]BR^{\rm SM}_{gg}}\left(1+\frac{\kappa_{\gamma\gamma}}{\frac{9}{16}A_W(\tau_W)+1}\right)^2 . \end{aligned} \tag{3.6}$$

The factor containing the SM branching $BR^{\rm SM}_{gg}$ takes into account the change in the Higgs total width due to the modification to the gluon couplings (while we neglect the effect of the photon channel in the total width). For other channels, we also finds similar equations with different efficiencies and branching ratios, as for instance the $H \to ZZ \to \ell^+\ell^-\ell^+\ell^-$ channel:

$$\mu_{ZZ} = \frac{(1+\kappa_{gg})^2 + \frac{\sum_{oth}\sigma_{oth}}{\sigma_{gg}}}{1+\frac{\sum_{oth}\sigma_{oth}}{\sigma_{gg}}}\frac{1}{1+\left[(1+\kappa_{gg})^2-1\right]BR^{\rm SM}_{gg}} . \tag{3.7}$$

Using the published CMS and ATLAS results, the result of the two parameter fit using κ_{gg} and $\kappa_{\gamma\gamma}$ is given in figure 1 using data from $\gamma\gamma$, ZZ and $\bar{b}b$ channels. One can see that the allowed region runs along the line A, which corresponds to SM cross section for the process $gg \to h \to \gamma\gamma$, even though largish values of κ_{gg} are excluded by the ZZ channel. As can be seen on the different contours, the current data already imposes a constraint on possible departures from the Standard Model point.

For reference, sample points for the following models are indicated:

- [♦] fourth generation, where the result is independent on the masses and Yukawa couplings. The point is given here for illustrative purposes; more complete fits on this case exist, see for example [24, 25];

JHEP03(2013)029

- [$*$] Littlest Higgs [26], where the result scales with the symmetry breaking scale f, set here to $f = 500\,\text{GeV}$ for a model with T-parity (there is also a mild dependence on the triplet VEV x, that we set $x = 0$);

- [▲] Simplest Little Higgs [27] (see section 4.2), where the result scales with the W' mass, also set here to $m_{W'} = 500\,\text{GeV}$ for a model with T-parity;

- [■] colour octet model [28], where the result is inversely proportional to the mass $m_S = 750\,\text{GeV}$ in the example (and also depends on two couplings set here to $\lambda_1 = 4$, $\lambda_2 = 1$);

- [⊗] 5D Universal Extra Dimension model [29], where only the top and W resonances contribute and the result scales with the size of the extra dimension (here we set $m_{KK} = 500\,\text{GeV}$ close to the experimental bound from electroweak precision tests);

- [★] 6D UED model on the Real Projective Plane [30, 31], with $m_{KK} = 600\,\text{GeV}$ is set to the LHC bound [32];

- [●] the Minimal Composite Higgs [33, 34] (Gauge Higgs unification in warped space) with the IR brane at $1/R' = 1\,\text{TeV}$, where only W and top towers contribute significantly and the point only depends on the overall scale of the KK masses, as the other parameters are fixed by the W and top masses;

- [▼] a flat (W' at 2 TeV) and [♠] warped ($1/R'$ at 1 TeV) version of brane Higgs models, in both cases the hierarchy in the fermionic spectrum is explained by the localisation, and all light fermion towers contribute; notwithstanding the many parameters in the fermion sector, the result only depends on the overall scale of the KK masses.

The numerical values of the parameters, whether including only κ_t or both κ_t and κ_W in the loop parameters, are given in table 5 for all the models listed above. The values are computed using the results in [2], while the 6D UED model has been computed in [35]. Note that the fit we present here is based on two independent parameters, while in many of the models we show all the parameters depend on a single model parameter, typically the mass scale of the new physics. Therefore, one should take any effective parameter fit with the caveat that the fit must be redone for a specific model taking into account the actual number of independent parameters in the BSM model. Note also that in all cases, except the fourth generation, the result scales with the mass of the new particles, therefore a point that falls in the exclusion region implies that a stronger bound on the mass of the new states is imposed by the Higgs measurements rather that the exclusion of the model. We should therefore think of the model as covering a line of points connecting the benchmark point in the figures with the origin (SM point).

The fit in figure 1 has been done using the χ^2 in eq. (3.2). In order to include the WW and $\bar{\tau}\tau$, we now use the improved χ^2. Thus we will focus on CMS data, and use ZZ and $\bar{b}b$ with likelihoods from eq. (3.2) (since we assume negligible change in $\bar{t}tH$ production, we can treat both channels as one dimensional distributions over the production modes) and WW, $\gamma\gamma$ and $\bar{\tau}\tau$ with likelihoods from eq. (3.3). We show the resulting contours in figure 2. By reducing to a two parameter fit on $\kappa'_{gg}, \kappa'_{\gamma\gamma}$ we make the assumption that k_Z is

JHEP03(2013)029

Model	parameter(s)	$\kappa_W - 1$	$\kappa'_{gg}(\kappa_t)$	$\kappa'_{\gamma\gamma}(\kappa_t)$	$\kappa'_{\gamma\gamma}(\kappa_t, \kappa_W)$
4^{th} generation	-	0	2	2	2
Simplest Little Higgs	$m_{W'} = 500\,\text{GeV}$	-0.009	-0.034	0.067	0.11
Littlest Higgs	$f = 700\,\text{GeV}$ $m_{W'} = 500\,\text{GeV}$, $x = 0$	-0.05	-0.11	-0.014	0.23
colour octet	$m_S = 750\,\text{GeV}$ $\lambda_1 = 4$, $\lambda_2 = 1$	0	0.37	0.17	0.17
5D UED	$m_{KK} = 500\,\text{GeV}$	0	0.20	0.034	0.034
6D UED (RP^2)	$m_{KK} = 600\,\text{GeV}$ ($R_5 = 1.5\ R_4$)	0	1.00	0.84	0.84
composite Higgs	$1/R' = 1\,\text{TeV}$	-0.04	-0.04	-0.03	0.14
flat brane Higgs	$m_{W'} = 2\,\text{TeV}$	-0.005	-0.45	-0.47	-0.45
warped brane Higgs	$1/R' = 1\,\text{TeV}$	-0.11	-0.65	-1.08	-0.57

Table 5. Higgs coupling parameters for various benchmark models: in parenthesis we indicate if κ_t and/or κ_W are included in the definition of the loop parameters. In the second column, the mass parameter the corrections are inversely proportional to (eventual other parameters are indicated in parenthesis). Here we only consider corrections to κ_W generated at tree level.

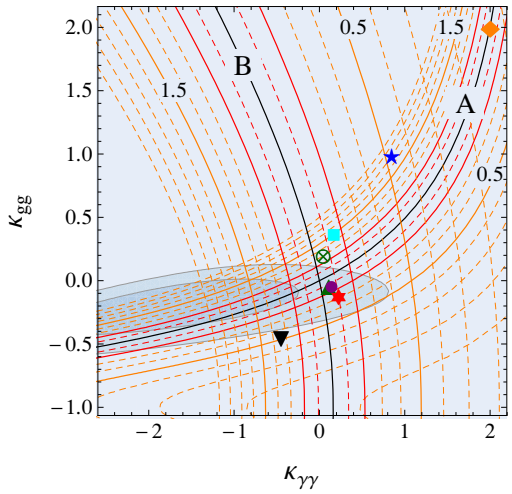

Figure 2. $\kappa'_{\gamma\gamma}$ and κ'_{gg} at the LHC for a Higgs boson with $m_H = 125\,\text{GeV}$. This plot use CMS data from all channels.

close to one, and that the changes in k_t, k_W are noticeable only in the loops, not in direct production or decays. All specific models fall into this category but the warped brane Higgs, which deviate significantly in k_W. To test this model, we will need to go beyond the 2-parameter fit.

3.3 Three parameter fit

As a sample and more general application of our parameterisation, we have also performed a three parameter fit, by adding to the two previous variables an explicit dependence on the gauge boson couplings. For simplicity, we assume that a custodial symmetry present

JHEP03(2013)029

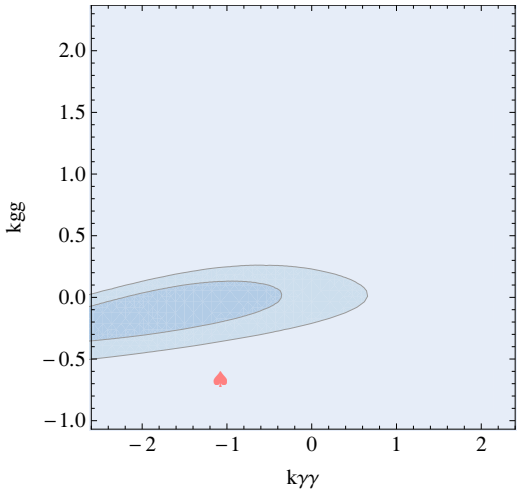

Figure 3. Three parameter fit at the LHC for a Higgs boson with $m_H = 125\,\text{GeV}$ using all channels from CMS. Here we present a slice of the allowed region for $\kappa_V = 0.89$. Darker (lighter) blue are the 1, 2 σ limits.

in the BSM models imposes $\kappa_Z = \kappa_W = \kappa_V$, so that we can treat deviations from the SM couplings of both W and Z with a single parameter. This is usually the case in any reasonable model of New Physics.

In the 3 parameter fit, the expression of the signal strengths in the $\gamma\gamma$ channel can be written as

$$\begin{aligned}\mu_{i,\,\gamma\gamma} &= \frac{(1+\kappa_{gg})^2\sigma^{\text{SM}}_{gg}\epsilon^i_{gg} + \kappa_V^2\left(\sigma^{\text{SM}}_{VBF}\epsilon^i_{VBF} + \sigma^{\text{SM}}_{ZH}\epsilon^i_{ZH} + \sigma^{\text{SM}}_{WH}\epsilon^i_{WH}\right)}{\sigma^{\text{SM}}_{gg}\epsilon^i_{gg} + \sigma^{\text{SM}}_{VBF}\epsilon^i_{VBF} + \sigma^{\text{SM}}_{ZH}\epsilon^i_{ZH} + \sigma^{\text{SM}}_{WH}\epsilon^i_{WH}} \times \frac{BR_{\gamma\gamma}}{BR^{\text{SM}}_{\gamma\gamma}} \\ &= \frac{(1+\kappa_{gg})^2\hat{\sigma}^i_{gg} + \kappa_V^2(1-\hat{\sigma}^i_{gg})}{1+(\kappa_V^2-1)(BR^{\text{SM}}_{WW+ZZ}) + [(1+\kappa_{gg})^2-1]\,BR^{\text{SM}}_{gg}}\left(1+\frac{\kappa_{\gamma\gamma}}{\frac{9}{16}A_W(\tau_W)+1}\right)^2 .\end{aligned} \tag{3.8}$$

For the ZZ channel:

$$\mu_{ZZ} = \frac{(1+\kappa_{gg})^2\sigma_{gg} + \kappa_V^2\sum_{oth}\sigma_{oth}}{\sigma_{gg}+\sum_{oth}\sigma_{oth}}\frac{\kappa_V^2}{1+(\kappa_V^2-1)(BR^{\text{SM}}_{WW+ZZ}) + [(1+\kappa_{gg})^2-1]\,BR^{\text{SM}}_{gg}} . \tag{3.9}$$

In figure 3 we present the results of the 3 parameter fit, by slicing the allowed region for $\kappa_V = 0.89$. This choice is motivated by the fact that this value correspond to the brane Higgs model in table 5. Thus we are taking the precise slice where the model lies, but one should not forget that we are dealing with a three parameter space. In particular the interpretation is different from a marginalisation over k_V. We see that the allowed region is very close to the one obtained in the 2 parameter fit in figure 2.

JHEP03(2013)029

4 Model interpretations

In general, the contribution of the new loops to the parameters can be written as [2]:

$$\kappa_{\gamma\gamma} = \sum_{NP} \frac{C^{\gamma}_{NP}}{C^{\gamma}_{t}} \frac{3}{4} N_{c,NP} Q^2_{NP}\, g_{hNP}\, \epsilon_{NP}\,, \tag{4.1}$$

$$\kappa_{gg} = \sum_{NP} \frac{C^{g}_{NP}}{C^{g}_{t}} 2C(r_{NP})\, g_{hNP}\, \epsilon_{NP}\,, \tag{4.2}$$

where $C^{\gamma}_{NP}/C^{\gamma}_{t}$ and C^{g}_{NP}/C^{g}_{t} are the NLO corrections normalised to the SM ones for the top in the $\gamma\gamma$-h and gluon-gluon-h triangle loop vertex, $N_{c,NP}$ is the number of colour components of the new states running in the loop, Q_{NP} is its electromagnetic charge, $C(r_{NP})$ is the Casimir of the colour representation of the new state ($C = 1/2$ for a fundamental), and ϵ_{NP} encodes the amplitude of the new physics loop. For masses of the state in the loop larger than the Higgs mass threshold, the amplitudes quickly asymptotise to a constant number that only depends on the spin of the state: this is already true with a very good precision for the top amplitude. Therefore, ϵ_{NP} can be simply approximated by a number dependent on the spin of the new states:

$$\begin{aligned} &\epsilon_{NP} = 1 && \text{for fermions}\,; \\ &\epsilon_{NP} = -21/4 && \text{for vectors}\,; \\ &\epsilon_{NP} = 1/4 && \text{for scalars}\,. \end{aligned} \tag{4.3}$$

The coupling of the new states to the Higgs is expressed in terms of the Higgs VEV dependence of the new state mass:

$$g_{hNP} = \frac{v}{m_{NP}} \frac{\partial m_{NP}(v)}{\partial v}\,. \tag{4.4}$$

Thus, in order to connect the new parameters κ_{gg} and $\kappa_{\gamma\gamma}$ to new physics models, it is enough to know the quantum numbers (charge, colour representation and spin) and the Higgs VEV dependent mass of the new particles. Eqs. 4.1 and 4.2 also allow to easily draw the correlation between the two parameters in specific models. For instance, in models with a single new particle:

$$\frac{\kappa_{\gamma\gamma}}{\kappa_{gg}} = \frac{3}{8} \frac{N_{c,NP} Q^2_{NP}}{C(r_{NP})}\,, \tag{4.5}$$

where we have assumed that the QCD corrections to the amplitudes are the same for the top and for new physics. For a top partner (i.e. a particle with the same quantum numbers as the top, except the spin):

$$\kappa_{\gamma\gamma} = \kappa_{gg}\,. \tag{4.6}$$

In most of the models listed in table 5, the result for the relevant parameters depends on a single mass scale (with just mild dependence on other parameters of the model).

JHEP03(2013)029

Therefore, the prediction cannot in principle be directly compared with any 2 or 3 (or more) parameter fit. For instance, when using the $\Delta\chi^2$ statistical test, one should compared it to a single parameter χ^2 distribution. However, the results obtained with an effective parameterisation, like the ones advocated here, can be used to give an indication if the data favours or disfavours the BSM model under consideration.

4.1 Higher-order corrections

It is a well known fact that Higgs physics (in the Standard Model as well as in many of its extensions) is largely affected by radiative corrections, in particular because of strong interactions. However, the exact calculation of those corrections is *a priori* model-dependent, which makes it impossible to include corrections in an effective Lagrangian without adding new parameters. In fact, higher order corrections can generate new operators or kinematic structures together with a simple re-scaling of the LO operators.

The parameterisation we propose, by splitting clearly the effect of tree level modification of tree level couplings and New Physics loop effects on the loop induced couplings, allows to easily add, at least partially, NLO corrections to the calculation. This is not a completely consistent procedure but the largest corrections are included. For instance, we have already seen that NLO QCD corrections to the top loop contribution to both gg-h and $\gamma\gamma$-h vertices factorise and give a simple multiplicative factor. We can expect that QCD corrections to the New Physics loops have the same structure and can be factorised: contributions of this type are already included in eqs. 4.1 and 4.2 via the factors C^{γ}_{NP} and C^{g}_{NP}. A precise and self-consistent calculation of such effects must be carried out in any given specific model. In the BSM model predictions in table 5, however, we assume that the QCD corrections are the same as in the SM top loop for simplicity. This is true for the contribution of coloured fermions (which is the most common case) because the corrections are independent on the mass of the fermion.

As already mentioned, this parameterisation cannot include NLO corrections that generate Lorentz structures different from the LO SM ones. For instance, electroweak 2-loop corrections to the gluon fusion cross sections, which are proportional to the coupling of the Higgs to W and Z, cannot be included [36]. Other corrections are loops involving both the production and decay process: such effects, however, are expected to be small because we are considering processes with the production of a Higgs boson in an s-channel resonance.

Anyway, even in an effective theory approach based on effective operators the procedure to compute radiative corrections implies adding new parameters to deal with the new structures. Indeed full consistency of the procedure can be guaranteed but this requires inserting counterterms [9]. From the point of view of a fit adding new parameters for describing a few per cent modification of the vertices is not necessarily an improvement. For example the two loop electroweak correction to $h \to \gamma\gamma$ is less than 2%, while the effect on $gg \to h$ is of order 5%.

JHEP03(2013)029

4.2 An example: the simplest little Higgs model

The new parameterisation offers an easy interpretation in terms of new physics models. The idea is that the contribution of new physics to the parameters will in general scale in a simple way with the mass of the new states: thus, any model will roughly cover a straight line originating at the origin (i.e. the SM point). By simply measuring the length of the excluded line, one can extract the bound on the new physics mass scale.

As an example, we present here the case of the Simplest Little Higgs model, described in section 3.3 of ref. [2]. The model contains both a W partner W' and a top partner T. Moreover, mixing between the two states generates a modification of the couplings of the Higgs to the SM W and top. Therefore, there will be a contribution to κ_W and κ_t from the modified tree level couplings, and to κ_{gg} and $\kappa_{\gamma\gamma}$ from the W' and T loops. From the W sector, the contributions are:

$$\kappa_W = 1 - \frac{1}{3}\frac{m_W^2}{m_{W'}^2}\,, \qquad \kappa_{\gamma\gamma}(W') = \frac{63}{16}\frac{m_W^2}{m_{W'}^2}\,, \qquad \kappa_{gg}(W') = 0\,. \tag{4.7}$$

Here $m_{W'}$ is the mass of the W' new particle. From the top sector, we have:

$$\kappa_t = 1 + \frac{m_t^2}{m_T^2} - \frac{4}{3}\frac{m_W^2}{m_{W'}^2}\,, \qquad \kappa_{gg}(T) = \kappa_{\gamma\gamma}(T) = -\frac{m_t^2}{m_T^2}\,. \tag{4.8}$$

As κ_t is not measurable, one can include its effects in the loop parameters (in this case, for illustration, we will leave κ_W in the fit, so we are intending a 3 parameter fit):

$$\kappa'_{gg}(k_t, T) = -\frac{4}{3}\frac{m_W^2}{m_{W'}^2}\,, \qquad \kappa'_{\gamma\gamma}(k_t, T, W') = \frac{125}{48}\frac{m_W^2}{m_{W'}^2}\,, \qquad \kappa_W - 1 = -\frac{1}{3}\frac{m_W^2}{m_{W'}^2}\,. \tag{4.9}$$

Thus:

- the parameters of the fit only depend on $m_W/m_{W'}$ and scale like $1/m_{W'}^2$ (this scaling is lost in the κ_g and κ_γ parameterisation);
- the correlation between the three parameters (in this model) is explicit, $\kappa_{gg} = -\frac{64}{125}\kappa_{\gamma\gamma} = -4(\kappa_W - 1)$.

This shows explicitly that specific model points (or regions) can be put in a global fit only for qualitative and illustrative purposes. In order to exclude a particular model at a given confidence level the χ^2 per degree of freedom should be calculate in the specific model, as in general this quantity is model dependent due to the fact that the supposedly independent fit parameters of a global analysis can be correlated in that specific model (in the example just given the three parameters reduce to only one independent parameter).

4.3 Fermiophobic Higgs model

In some cases, models are not represented by single points but still contain parameters that we can directly cast in our parameterisation. For instance, we consider here a class of models in which fermions do not couple to the Higgs boson and, therefore, all the Higgs

JHEP03(2013)029

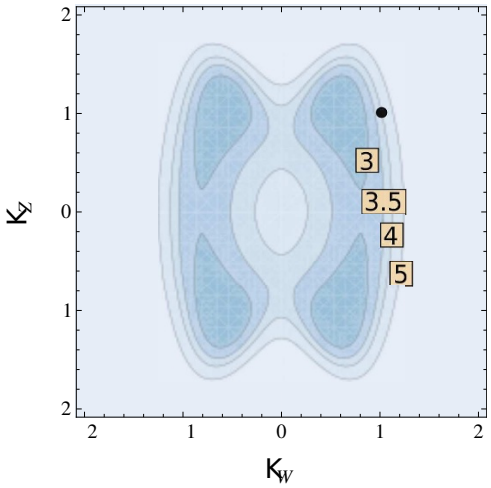

Figure 4. Fermiophobic Higgs model fit at the LHC with $m_H = 125\,\text{GeV}$ using all channels from CMS, in the $(\kappa_W,\ \kappa_Z)$ plane. Darker (lighter) blue are the 3, 3.5, 4 and 5 σ regions. The black dot labels the fermiophobic SM, $\kappa_W = \kappa_Z = 1$.

phenomenology takes place via the couplings to vectors. As a consequence, the main decay channel $\bar{b}b$ disappears, as well as the main production mode, $gg \to h$ (occurring only through fermion loops). These two combined effects leave the inclusive cross-sections for bosonic channels not too different from the SM expectations. The overall effect of this new physics is included in the couplings of the Higgs boson to the W and Z bosons, through the coefficients κ_W and κ_Z. All fermionic κ_f are therefore set to zero, together with κ_{gg} and $\kappa_{\gamma\gamma}$. We do not assume custodial symmetry in order to be able to probe all possible models in the two dimensional (κ_W, κ_Z) parameter space.

Apparently, this class of models precludes the use of the improved χ^2 method described in section 3.1, since VBF and VH production are not rescaled in the same way. However it is possible to include the WW channel by noting that this channel is still quite insensitive to VBF production mode (this is demonstrated in the CMS analysis [37]). Concerning the $\bar{\tau}\tau$ channel, since this Higgs is fermiophobic, the signal is set to zero and therefore all production channels become irrelevant: in particular, we will have $\mu_{VBF} = \mu_{VH} = 0$ throughout the whole (κ_W, κ_Z) plane, thus this satisfies the requirement for the use of the improved χ^2. In this case it turns out that the p-value of the best fit is low ($3.7\ 10^{-3}$), hence the $\Delta\chi^2$ test tends to be weaker than what is usually expected. Thus we have used here an approximate χ^2 test instead, which explains why there is no 1 and 2 sigmas contours. The result is shown in figure 4: it shows a four-fold degeneracy of the χ^2 region with respect to the parameter space due to the obvious sign degeneracy of the two tree-level couplings. The black point corresponding to a fermiophobic Standard Model is excluded by more than 3.5 sigmas.

4.4 Dilaton model

Another interesting class of models is represented by dilatons, which can play the role of an impostor of the Higgs. A dilaton can be thought of as a Pseudo-Nambu-Goldstone boson associated with an approximate scale invariance: it can give rise to phenomenology

JHEP03(2013)029

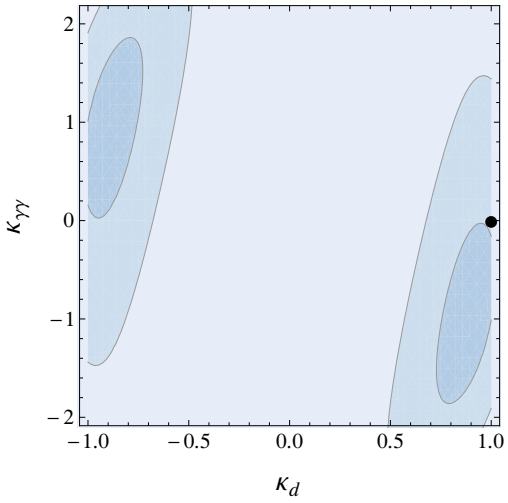

Figure 5. Dilatonic model fit at the LHC for a Higgs boson with $m_H = 125\,\text{GeV}$ using all channels from CMS. Here we present the allowed region in a slice $\kappa_{gg} = 0$, in the $(\kappa_d, \kappa_{\gamma\gamma})$ plane. Darker (lighter) blue are the 1, 2 σ regions.

at colliders analogous to the one of a Higgs boson because it is expected to couple with the terms that break scale invariance, i.e. mass terms [38, 39]. Therefore, it can mimick a Higgs boson in Higgs-less models [40], or modifying the couplings of a standard-like Higgs boson via mixing [41]. Dilatons are for example present in all extra-dimensional models, where they are associated with the compactification of the extra space dimensions, and in technicolour models, where they may appear as light scalar degrees of freedom of the confining theory [42, 43]. They have already been indicated as possible impostors of the Higgs.

In this section, we will study a simplified dilaton model, where the impersonator has couplings to all massive states in the SM equal to the SM Higgs boson up to a rescaling factor $\kappa_d = v/f$, where v is the SM Higgs vacuum expectation value, and f is the scale associated with the breaking of the scale invariance (typically one expects $f > v$). The model under consideration, therefore, has equal tree level couplings $\kappa_W = \kappa_Z = \kappa_f = \kappa_d$. Production cross sections and decay widths are accordingly modified, which allows us to get constraints on κ_d. We still study here in addition to this κ_d, the influence of new physics entering the loops, giving κ_{gg} and $\kappa_{\gamma\gamma}$ coefficients, and thus perform a 3 parameter fit. We use here again the χ^2 statistical test. In figure 5 we show a slice of the parameter space for $\kappa_{gg} = 0$, which includes the SM Higgs point ($\kappa_d = 1$, $\kappa_{\gamma\gamma} = 0$). The standard model like case is consistent with the fit on the CMS data within a bit more than 1 sigma, as expected. The best fit corresponds to a slightly smaller values of $|\kappa_d| < 1$, however with new physics in the Higgs to $\gamma\gamma$ loop (when assuming $\kappa_{gg} = 0$). In any case there is neither strong exclusion nor strong indication for such a dilation scenario in present data: the only information we can extract is that small values of $\kappa_d \ll 1$ are disfavoured, even by allowing for arbitrary new physics contributions in the loops. If this conclusion were to hold a stronger statistical significance, any model of dilatons described by our simplified parameterisation would be excluded.

JHEP03(2013)029

5 Conclusion

We have discussed a generalisation of the parameterisation proposed in [2] to include tree-level couplings and we showed how it can be used for testing and putting exclusion limits on models of new physics beyond the Standard Model. The most important radiative corrections, involving QCD NLO corrections, can be easily included in this parameterisation. We have compared this formalism to other parameterisations, in particular the one proposed in [1]. We showed that the two, while sharing the same tree-level structure, are fundamentally different concerning the treatment the the loop-level couplings. In particular while the parameters in [1] are inspired from the experimentally measured quantities, our parameterisation is tailored to investigate BSM models, keeping track of the specific correlations among the parameters. It also allows more easily to interpret mass limits and contributions to the loops giving the effective Higgs boson vertices. In fact, the parameters we propose are easily calculable in extensions of the Standard Model, and we clearly see in the plots that different models cluster in specific directions in the κ_{gg} and $\kappa_{\gamma\gamma}$ parameter space. This property is due to our choice to normalise the New Physics loop to the SM top one. We also performed 2 parameter fits of the CMS and ATLAS results in the $H \to \gamma\gamma$, $H \to ZZ$ and $H \to b\bar{b}$ channels and 2 and 3 parameter fits using all available channels, showing that the 2 and 3 parameter fits already include all the necessary information and are therefore a good approximation at this stage. More precise measurements of extra channels will require the inclusion of more effective parameters. We have also given few example of possible dedicated fits of BSM models: a little Higgs model, a fermiophobic model and a dilation model, testing in all these cases the relevant parameters space with a χ^2 test using available data. We hope that this work will trigger interest of adding the proposed parameterisation to the existing ones in performing experimental fits on data by the ATLAS and CMS collaborations concerning the Higgs boson.

Acknowledgments

We thank L. Panizzi for discussions and for suggesting the fit of the fermiophobic Higgs model. We also thank S. Shotkin-Gascon, N. Chanon and the CMS group in Lyon for useful discussions.

References

[1] LHC Higgs Cross section Working Group, A. David et al., *LHC HXSWG interim recommendations to explore the coupling structure of a Higgs-like particle*, arXiv:1209.0040 [INSPIRE].

[2] G. Cacciapaglia, A. Deandrea and J. Llodra-Perez, *Higgs $\to \gamma\gamma$ beyond the standard model*, *JHEP* **06** (2009) 054 [arXiv:0901.0927] [INSPIRE].

JHEP03(2013)029

[3] F. Bonnet, M. Gavela, T. Ota and W. Winter, *Anomalous Higgs couplings at the LHC and their theoretical interpretation*, *Phys. Rev.* **D 85** (2012) 035016 [arXiv:1105.5140] [INSPIRE].

[4] F. Bonnet, T. Ota, M. Rauch and W. Winter, *Interpretation of precision tests in the Higgs sector in terms of physics beyond the standard model*, *Phys. Rev.* **D 86** (2012) 093014 [arXiv:1207.4599] [INSPIRE].

[5] T. Corbett, O. Eboli, J. Gonzalez-Fraile and M. Gonzalez-Garcia, *Constraining anomalous Higgs interactions*, *Phys. Rev.* **D 86** (2012) 075013 [arXiv:1207.1344] [INSPIRE].

[6] J. Espinosa, C. Grojean, M. Muhlleitner and M. Trott, *Fingerprinting Higgs suspects at the LHC*, *JHEP* **05** (2012) 097 [arXiv:1202.3697] [INSPIRE].

[7] J. Espinosa, C. Grojean, M. Muhlleitner and M. Trott, *First glimpses at Higgs' face*, *JHEP* **12** (2012) 045 [arXiv:1207.1717] [INSPIRE].

[8] G. Bélanger et al., *Higgs bosons at* 98 *and* 125 *GeV at LEP and the LHC*, *JHEP* **01** (2013) 069 [arXiv:1210.1976] [INSPIRE].

[9] G. Passarino, *NLO inspired effective lagrangians for Higgs physics*, *Nucl. Phys.* **B 868** (2013) 416 [arXiv:1209.5538] [INSPIRE].

[10] G. Bélanger, B. Dumont, U. Ellwanger, J. Gunion and S. Kraml, *Higgs couplings at the end of 2012*, *JHEP* **02** (2013) 053 [arXiv:1212.5244] [INSPIRE].

[11] G. Moreau, *Constraining extra-fermion(s) from the Higgs boson data*, *Phys. Rev.* **D 87** (2013) 015027 [arXiv:1210.3977] [INSPIRE].

[12] M. Spira, A. Djouadi, D. Graudenz and P. Zerwas, *Higgs boson production at the LHC*, *Nucl. Phys.* **B 453** (1995) 17 [hep-ph/9504378] [INSPIRE].

[13] A. Azatov, R. Contino and J. Galloway, *Model-independent bounds on a light Higgs*, *JHEP* **04** (2012) 127 [arXiv:1202.3415] [INSPIRE].

[14] CMS collaboration, *Evidence for a new state decaying into two photons in the search for the standard model Higgs boson in pp collisions*, CMS-PAS-HIG-12-015 (2012).

[15] https://twiki.cern.ch/twiki/bin/view/CMSPublic/PhysicsResultsHIG.

[16] ATLAS collaboration, *Observation of an excess of events in the search for the Standard Model Higgs boson in the gamma-gamma channel with the ATLAS detector*, ATLAS-CONF-2012-091 (2012).

[17] LHC Higgs Cross section Working Group, *Higgs cross sections at* 7, 8 *and* 14 *TeV*, https://twiki.cern.ch/twiki/bin/view/LHCPhysics/CrossSections.

[18] CMS collaboration, *Evidence for a new state in the search for the standard model Higgs boson in the* $H \to ZZ \to 4$ *leptons channel in pp collisions at* $\sqrt{s} = 7$ *and* 8 *TeV*, CMS-PAS-HIG-12-016 (1460664).

[19] ATLAS collaboration, *Observation of an excess of events in the search for the standard model Higgs boson in the* $H \to ZZ^{(*)} \to 4l$ *channel with the ATLAS detector*, ATLAS-CONF-2012-092 (2012).

[20] CMS collaboration, *Search for the standard model Higgs boson produced in association with W or Z bosons, and decaying to bottom quarks for HCP 2012*, CMS-PAS-HIG-12-044 (2012).

JHEP03(2013)029

[21] ATLAS collaboration, *Search for the Standard Model Higgs boson produced in association with a vector boson and decaying to bottom quarks with the ATLAS detector*, ATLAS-CONF-2012-161 (2012).

[22] CMS collaboration, *Combination of standard model Higgs boson searches and measurements of the properties of the new boson with a mass near* 125 *GeV*, CMS-PAS-HIG-12-045 (2012).

[23] ATLAS collaboration, *Coupling properties of the new Higgs-like boson observed with the ATLAS detector at the LHC*, ATLAS-CONF-2012-127 (2012).

[24] A. Djouadi and A. Lenz, *Sealing the fate of a fourth generation of fermions*, *Phys. Lett.* **B 715** (2012) 310 [arXiv:1204.1252] [INSPIRE].

[25] O. Eberhardt et al., *Impact of a Higgs boson at a mass of* 126 *GeV on the standard model with three and four fermion generations*, *Phys. Rev. Lett.* **109** (2012) 241802 [arXiv:1209.1101] [INSPIRE].

[26] N. Arkani-Hamed, A. Cohen, E. Katz and A. Nelson, *The littlest Higgs*, *JHEP* **07** (2002) 034 [hep-ph/0206021] [INSPIRE].

[27] M. Schmaltz, *The simplest little Higgs*, *JHEP* **08** (2004) 056 [hep-ph/0407143] [INSPIRE].

[28] A.V. Manohar and M.B. Wise, *Flavor changing neutral currents, an extended scalar sector and the Higgs production rate at the CERN LHC*, *Phys. Rev.* **D 74** (2006) 035009 [hep-ph/0606172] [INSPIRE].

[29] T. Appelquist, H.-C. Cheng and B.A. Dobrescu, *Bounds on universal extra dimensions*, *Phys. Rev.* **D 64** (2001) 035002 [hep-ph/0012100] [INSPIRE].

[30] G. Cacciapaglia, A. Deandrea and J. Llodra-Perez, *A dark matter candidate from Lorentz invariance in 6D*, *JHEP* **03** (2010) 083 [arXiv:0907.4993] [INSPIRE].

[31] A. Arbey, G. Cacciapaglia, A. Deandrea and B. Kubik, *Dark matter in a twisted bottle*, *JHEP* **01** (2013) 147 [arXiv:1210.0384] [INSPIRE].

[32] G. Cacciapaglia and B. Kubik, *Even tiers and resonances on the real projective plane*, *JHEP* **02** (2013) 052 [arXiv:1209.6556] [INSPIRE].

[33] K. Agashe, R. Contino and A. Pomarol, *The minimal composite Higgs model*, *Nucl. Phys.* **B 719** (2005) 165 [hep-ph/0412089] [INSPIRE].

[34] K. Agashe and R. Contino, *The minimal composite Higgs model and electroweak precision tests*, *Nucl. Phys.* **B 742** (2006) 59 [hep-ph/0510164] [INSPIRE].

[35] K. Nishiwaki, K.-y. Oda, N. Okuda and R. Watanabe, *A bound on universal extra dimension models from up to* $2\,fb^{-1}$ *of LHC data at* 7 *TeV*, *Phys. Lett.* **B 707** (2012) 506 [arXiv:1108.1764] [INSPIRE].

[36] U. Aglietti, R. Bonciani, G. Degrassi and A. Vicini, *Two loop light fermion contribution to Higgs production and decays*, *Phys. Lett.* **B 595** (2004) 432 [hep-ph/0404071] [INSPIRE].

[37] CMS collaboration, *Evidence for a particle decaying to* W^+W^- *in the fully leptonic final state in a standard model Higgs boson search in pp collisions at the LHC*, CMS-PAS-HIG-12-042 (2012).

[38] W.D. Goldberger, B. Grinstein and W. Skiba, *Distinguishing the Higgs boson from the dilaton at the Large Hadron Collider*, *Phys. Rev. Lett.* **100** (2008) 111802 [arXiv:0708.1463] [INSPIRE].

JHEP03(2013)029

[39] J. Fan, W.D. Goldberger, A. Ross and W. Skiba, *Standard Model couplings and collider signatures of a light scalar*, *Phys. Rev.* **D 79** (2009) 035017 [arXiv:0803.2040] [INSPIRE].

[40] C. Csáki, J. Hubisz and S.J. Lee, *Radion phenomenology in realistic warped space models*, *Phys. Rev.* **D 76** (2007) 125015 [arXiv:0705.3844] [INSPIRE].

[41] M. Battaglia, S. De Curtis, A. De Roeck, D. Dominici and J.F. Gunion, *On the complementarity of Higgs and radion searches at LHC*, *Phys. Lett.* **B 568** (2003) 92 [hep-ph/0304245] [INSPIRE].

[42] D. Elander, C. Núñez and M. Piai, *A light scalar from walking solutions in gauge-string duality*, *Phys. Lett.* **B 686** (2010) 64 [arXiv:0908.2808] [INSPIRE].

[43] T. Appelquist and Y. Bai, *A light dilaton in walking gauge theories*, *Phys. Rev.* **D 82** (2010) 071701 [arXiv:1006.4375] [INSPIRE].

JHEP03(2013)029